THE JOURNAL OF COMPARATIVE NEUROLOGY 402:419–434 (1998)

Chemical Anatomy of the Macaque Monkey Olfactory Bulb: NADPH-Diaphorase/Nitric Oxide Synthase Activity

JOSÉ R. ALONSO,* A. PORTEROS, C. CRESPO, R. ARÉVALO, J.G. BRIÑÓN, E. WERUAGA, AND J. AIJÓN
Universidad de Salamanca, Departamento de Biología Celular y Patología, 37007 Salamanca, Spain

ABSTRACT

The distribution and the morphology of nicotinamide adenine dinucleotide phosphate (NADPH)-diaphorase (ND)-active and neuronal nitric oxide synthase (NOS)-immunoreactive neurons and fibers were studied in the olfactory bulb of three species of primates, i.e., the cynomolgus macaque monkey (*Macaca fascicularis*), the Japanese macaque monkey (*Macaca fuscata),* and the pig-tail macaque monkey (*Macaca nemestrina*). The ND staining was carried out by means of a direct histochemical method with β-NADPH as cosubstrate and nitro blue tetrazolium as chromogen. The NOS immunostaining was carried out by using a polyclonal antibody and the avidin-biotin peroxidase method. Similar results were found in the three species, where a distinct distribution pattern of ND/NOS-stained neurons and fibers was observed. All olfactory fibers demonstrated ND-positive labeling but they were NOS-immunonegative. In the superficial modulatory area of the olfactory bulb, a few weakly ND- and NOS-positive periglomerular cells, stellate cells, and darkly stained superficial short-axon cells were observed. In the inframitral layers, granule cells, deep stellate cells, and deep short-axon cells were distinguished. Short-axon cells had oriented morphologies and spiny dendrites. Many thick, varicose ND/NOS-stained fibers identified as centrifugal fibers were observed in the white matter, granule cell layer, internal plexiform layer, mitral cell layer, and external plexiform layer. This distribution of ND activity and NOS immunoreactivity showed similarities to and differences from what has been reported in the olfactory bulb of macrosmatic mammals including rodents (rat, mouse, and hamster) and insectivores (hedgehog). These data confirm that the complexity of the ND/NOS staining in the olfactory bulb of one species correlates with the importance of olfaction in the biology of such species. J. Comp. Neurol. 402:419–434, 1998.

Indexing terms: histochemistry; immunohistochemistry; olfaction; primate

Reduced nicotinamide adenine dinucleotide phosphate (NADPH) diaphorase is an oxidoreductase enzyme that can be detected in a histochemical reaction by incubating fixed brain sections in a buffered solution containing β-NADPH as cosubstrate and a tetrazolium salt as chromogen (Pearse, 1972; Kiernan, 1990). The enzyme NADPH-diaphorase (ND) is a selective histochemical marker for distinct neuronal populations throughout the brain (Scott et al., 1987; Villalba et al., 1988, 1989; Mizukawa et al., 1989; Bredt et al., 1991a; Davis, 1991; Vincent and Kimura, 1992; Kishimoto et al., 1993; Alonso et al., 1993, 1995a,b; Hopkins et al., 1996; Briñón et al., 1997; among others). After being purified and molecularly cloned from brain, neuronal nitric oxide synthase (NOS) has been found in discrete neuronal populations in the rodent and primate brains, and its localization is coincident with ND staining in both groups of mammals after aldehyde fixation (Bredt et al., 1991a). The ND has been subsequently identified as a nitric oxide synthase (Hope et al., 1991), although there are a few locations, including the olfactory receptor cells,

Grant sponsor: Junta de Castilla y León; Grant sponsor: DGES; Grant numbers: PB97–1341, HA-135.

*Correspondence to: Dr. José R. Alonso, Dpto. Biología Celular y Patología, Universidad de Salamanca, E-37007 Salamanca, Spain. E-mail: jralonso@gugu.usal.es

Received 6 April 1998; Revised 13 August 1998; Accepted 25 August 1998

where ND labels cytochrome P450 reductase (Kishimoto et al., 1993), an enzyme with a close homology with NOS (Bredt et al., 1991b).

The chemical anatomy of the olfactory bulb (OB) has been extensively studied because of its clear lamination, well-known neuronal typology, easy experimental access, and large diversity of neurotransmitters and neuroactive substances. Although the OB cytoarchitecture is remarkably constant among vertebrates (Allison, 1953), there are significant variations on its anatomical and functional organization between macrosmatic and microsmatic animals (Takagi, 1981, 1984, 1986; Mestre et al., 1992). The chemoarchitecture of the OB demonstrates a considerable interspecies variability (Takeuchi et al., 1982; Baker, 1986; Matsutani et al., 1989; Baker et al., 1991; Davis, 1991; Alonso et al., 1995b), although some neurochemically identified populations are similar in microsmatic and macrosmatic mammals (Sanides-Kohlrausch and Wahle, 1991; Bassett et al., 1992). Whereas the neuronal circuitry in the OB of macrosmatic animals has been extensively studied, less information is available about the OB in microsmatic animals, especially in human and nonhuman primates. ND and NOS may be valuable tools in the characterization of specific neuronal and fiber populations in the macaque olfactory bulb, because cells positive for ND and NOS are frequently stained in a Golgi-like way, showing in extensive detail the dendritic and axonal processes.

Even though several studies detailing the distribution and morphological characteristics of ND-active and NOS-immunoreactive neurons and fibers have been carried out in the OB of mammals (rat: Scott et al., 1987; Villalba et al., 1988, 1989; Davis, 1991; Vincent and Kimura, 1992; Alonso et al., 1993; Porteros et al., 1994; Hopkins et al., 1996; Briñón et al., 1997; hamster: Davis, 1991; mouse: Kishimoto et al., 1993; hedgehog: Alonso et al., 1995b), no information is available for nonhuman primates. From those studies, interspecies differences can be deduced, even for phylogenetically close species such as hamster and rat (Davis, 1991). These differences were more pronounced between rodents and the hedgehog, an insectivorous with an extraordinary development of the olfactory structures (Alonso et al., 1995b).

The aims of this study were to map in detail the distribution and morphological features of ND/NOS-positive elements (neurons and fibers) in the macaque OB, and to compare these data with previous observations on ND and NOS activities in the OB of other groups of vertebrates.

Abbreviations

AOB	accessory olfactory bulb
DSA	deep short-axon cell
DSC	deep stellate cell
EPL	external plexiform layer
GC	granule cell
GCL	granule cell layer
GL	glomerular layer
HZ	horizontal cell
IPL	internal plexiform layer
MCL	mitral cell layer
NADPH	nicotinamide adenine dinucleotide phosphate, reduced form
ND	NADPH-diaphorase
NOS	neuronal nitric oxide synthase
OB	olfactory bulb
ONL	olfactory nerve layer
OP	olfactory peduncle
PG	periglomerular cell
SSA	superficial short-axon cell
SSC	superficial stellate cell
WM	white matter

MATERIALS AND METHODS

Animals and tissue preparation

Four adult male cynomolgus monkeys (*Macaca fascicularis*) weighing between 2.7 and 3.8 kg, seven adult Japanese macaques (*Macaca fuscata*) weighing between 2.8 and 3.6 kg, and five adult male pig-tail monkeys (*Macaca nemestrina*) weighing between 4.5 and 6.5 kg were used. The macaque monkey olfactory bulbs were donated by different groups working in the neuroanatomy of other parts of the brain (see Acknowledgments). In all cases, pertinent authorization for the utilization of the animal was obtained from the corresponding ethical committees. The brains of these animals were used in other neuroanatomical studies, not related with the olfactory system. For comparison of the general cytoarchitecture of the OB between rodents and macaque monkeys, we used Nissl-stained coronal sections of the rat OB. For this purpose, material from previous studies (female Wistar rats weighing between 200 and 250 g) was used. All procedures were in accordance with the guidelines of the European Communities Directive (86/609/EEC), the current Spanish legislation for the use and care of animals, and conform to NIH guidelines. This particular study was also approved by the Animal and Human Experimentation Committee of the Institute of Neuroscience of Castilla y León (INCyL).

The cynomolgus monkeys were tranquilized with ketamine-HCl (10 mg/kg, i.m.) and deeply anesthetized with sodium pentobarbital (50 mg/kg, i.p.). After rinsing the vascular tree with 500 ml of 0.9% saline, the following fixatives were transcardially perfused: 4% paraformaldehyde in 0.1 M sodium acetate buffer, pH 6.5 (250 ml/min for 5 minutes and 100 ml/minute for 15 minutes), and 4% paraformaldehyde in 0.1 M sodium borate buffer, pH 9.5 (100 ml/minute for 30 minutes). The olfactory bulbs were dissected out and postfixed in the same fixative for 6 hours at 4°C. The pig-tail monkeys and the Japanese macaque monkeys were anesthetized with Nembutal and ketamine-HCl (10 mg/kg, i.m.). The vascular tree was rinsed with 0.8–1 l of 0.9% saline, followed by the perfusion of 4–5 liters of 4% paraformaldehyde in 0.1 M phosphate buffer, pH 7.3 (PB). After dissection, the olfactory bulbs were postfixed in the same fixative during 2–6 hours at 4°C. Wistar rats were anaesthetized with ketamine (Ketolar, 50 mg/kg body weight). The vascular tree was rinsed with 100 ml of 0.9% saline, followed by the perfusion of 400 ml of 4% paraformaldehyde and 2% picric acid in PB. After dissection, the olfactory bulbs were postfixed in the same fixative during 4 hours at 4°C.

After washing in PB, the olfactory bulbs were cryoprotected in either 30% sucrose or 20% glycerol with 2% dimethyl sulfoxide (DMSO) in PB for 1 day. The olfactory bulbs were frozen with cooled isopentane (Rosene et al., 1986) and stored at −70°C until further processing. Serial sections were cut at 30 μm at the coronal or sagittal plane with a freezing, sliding microtome. Until the histochemical staining, the sections were stored in tissue collecting solution (30% ethylene glycol and 25% glycerin in 0.05 M sodium phosphate buffer, pH 7.3) at −20°C.

Nissl staining

Sections were rinsed in PB and postfixed in buffered formalin (pH 7.4) for 10 days. After mounting on gelating-coated slides, lipids were eliminated with a chloroform-ethanol solution (1:1) for 2 hours. Sections were rehydrated in graded ethanol series and stained with 0.25% thionin at 37°C for 10 minutes. Sections were dried overnight at 37°C, dehydrated through graded ethanol series, cleared with xylene, and coverslipped with DPX or Entellan. The sections were stored in the dark until analyzed.

ND histochemistry

The sections were rinsed in 0.1 M Tris-HCl buffer (pH 8.0) at room temperature and incubated for 45 minutes at 37°C with mild agitation in a solution made up of 1.2 mM β-NADPH (Sigma #N-1630), 0.3 mM nitro blue tetrazolium (Sigma #N-6876) dissolved in DMSO (the final DMSO concentration in the incubation mixture was 2.5%), and 0.1% Triton X-100 in 0.1 M Tris-HCl buffer, pH 8.0. The reaction was controlled under the microscope. When the histochemical reaction was concluded, the sections were rinsed (3 × 10 minutes) in cold 0.1 M sodium phosphate buffer (pH 7.4), and mounted onto gelatin-coated slides from 0.05 M phosphate buffer (pH 7.4). They were dried overnight at 37°C, dehydrated through ethanol series, cleared with xylene, and coverslipped with DPX or Entellan. The sections were stored in the dark until analyzed.

In order to determine the specificity of the histochemical reaction, controls as described (Alonso et al., 1995a) were carried out: 1) incubation without the substrate β-NADPH; 2) incubation without the chromogen nitro blue tetrazolium in order to rule out possible nonspecific formation of reaction product; 3) heat denaturation of the enzyme activity by heating the tissue at 84°C for 5 minutes; and 4) overfixation of tissue (2 weeks in 10% formalin). In all cases, no residual reaction was observed.

NOS immunocytochemistry

Sections were rinsed in PB and processed for immunohistochemistry by using the avidin-biotin-peroxidase method. The sections were sequentially incubated in: 1) primary antibody (K205 sheep anti-rat NOS antibody, gift from Drs. Charles and Emson, Cambridge, U.K.) diluted 1:20,000 in PB containing 10% normal horse serum and 0.03% Triton X-100 for 48 hours at 4°C; 2) biotinylated anti-sheep IgG (Vector Labs., Burlingame, CA) diluted 1:250 in PB for 2 hours at room temperature; and 3) horseradish peroxidase-coupled avidin complex (1:200 in PB, Vector) for 2 hours at room temperature. The peroxidase was visualized with 0.07% 3,3'diaminobenzidine and 0.003% hydrogen peroxide in 0.1 M Tris-HCl buffer (pH 7.6). The sections were stored in the dark until analyzed.

Control experiments were carried out by incubating sections in the absence of primary antibody, secondary antibody, or avidin-peroxidase complex. No immunostaining was detected. Furthermore, the specificity of the antiserum has been previously described (Herbison et al., 1996). This antibody recognizes NOS in Western blots, and the immunoreactivity is abolished by absorption of the K205 antiserum with recombinant NOS protein.

TABLE 1. ND/NOS-Positive Neuronal Types in the *Macaca nemestrina* Olfactory Bulb[1]

Cell type	ND-staining[2]	Max. diameter µm (mean ± SEM)	Location	Frequency[3]
Periglomerular cell	Weak (type III)	9.57 ± 0.13	GL[4]	++
Superficial short-axon cell	Strong (type I)	21.69 ± 0.41	GL/EPL	+
Superficial stellate cell	Weak (type II)	14.46 ± 0.27	GL/EPL	+
Granule cell	Weak (type III)	7.95 ± 0.28	GCL	+++
Deep stellate cell	Weak (type II)	14.44 ± 0.52	GCL	+
Deep short-axon cell	Strong (type I)	24.97 ± 1.10	GCL/WM	++

[1]ND/NOS, NADPH diaphorase/nitric oxide synthase.
[2]ND-active types according to Mizukawa et al. (1989).
[3]Frequency: +++, more than 10 cells per section; ++, 1 to 10 cells per section; +, less than 1 cell per section.
[4]EPL, external plexiform layer; GCL, granule cell layer; GL, glomerular layer; WM, white matter.

Analysis

Sections were analyzed by using brightfield (cells and fibers) and darkfield (fibers) condensers with 16×, 25×, 40×, and 100× planapochromatic objectives (Zeiss, Thornwood, NY). Photographs of positive cell types were taken with a Zeiss III or Zeiss Axiophot photomicroscopes.

For the quantitative analysis, we used the olfactory bulbs from *Macaca nemestrina* because series of these sections were processed simultaneously under the same incubation conditions. The cell diameters of individual labeled cells were drawn with a camera lucida using a 100× oil immersion objective, and plotted on a digitizer tablet connected to a semiautomatic image analysis system (MOP-Videoplan, Kontron, Munich). For the measurement of cell sizes of weakly labeled neurons, only cells in which the nucleus was clearly visible were used. In the darkly stained neuronal types where the dense colored precipitate masked the nucleus, the chosen neurons were those located in the middle of the thickness of the section and showing at least two primary dendrites. For each neuronal type, 300 cells from all five animals were measured. When the labeled cell type was scarce (+ in Table 1), all labeled neurons, always over 50 cells, were included in the quantification.

RESULTS

General structure of the monkey olfactory bulb

The OB of the macaque monkey is a laminar structure where seven layers can be differentiated (Figs. 1, 2). All three species used shared a common laminar pattern. The nomenclature developed by Ramón y Cajal (1904) for the OB of macrosmatic mammals can be used because the same layers are present and their limits are easily discernible. According to this nomenclature, from most external to most internal, the following layers are distinguished: olfactory nerve layer (ONL), glomerular layer (GL), external plexiform layer (EPL), mitral cell layer (MCL), internal plexiform layer (IPL), granule cell layer (GCL), and white matter (WM; Fig. 1). Nevertheless, there are some differences in the lamination between primates and rodents. In rodents, mitral cells are densely packed in a narrow monolayer, whereas in the monkey, the MCL is less defined and the cell bodies of the mitral cells are disposed at different levels, and the neuropil between them is more abundant (Fig. 2). Another difference is observed in the

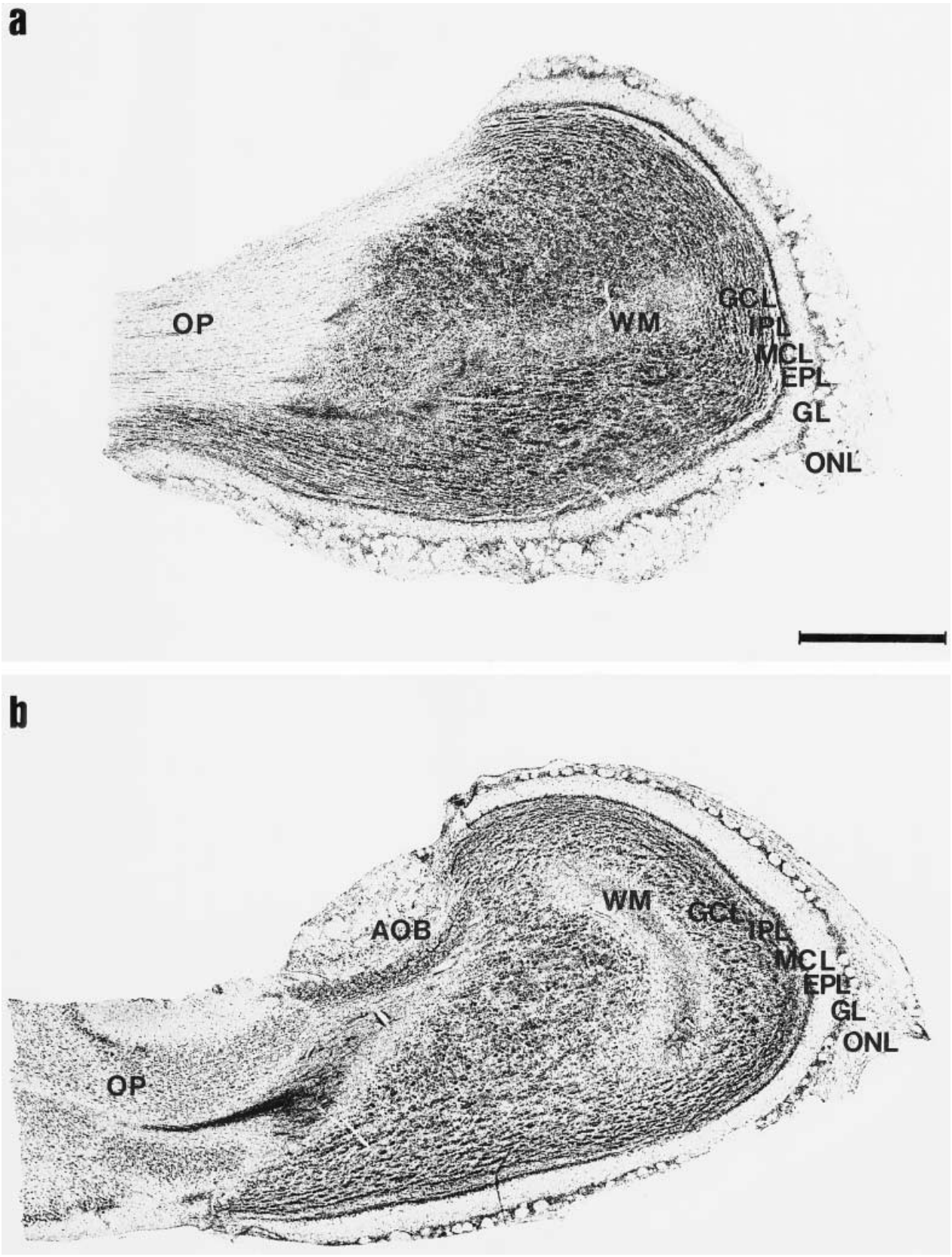

Fig. 1. Parasagittal Nissl-stained sections showing the general organization of olfactory bulb in *Macaca fuscata* (**a**) and rat (**b**). AOB, accessory olfactory bulb; GCL, granule cell layer; GL, glomerular layer; EPL, external plexiform layer; IPL, internal plexiform layer; MCL, mitral cell layer; ONL, olfactory nerve layer; OP, olfactory peduncle; WM, white matter. Scale bar = 1 mm.

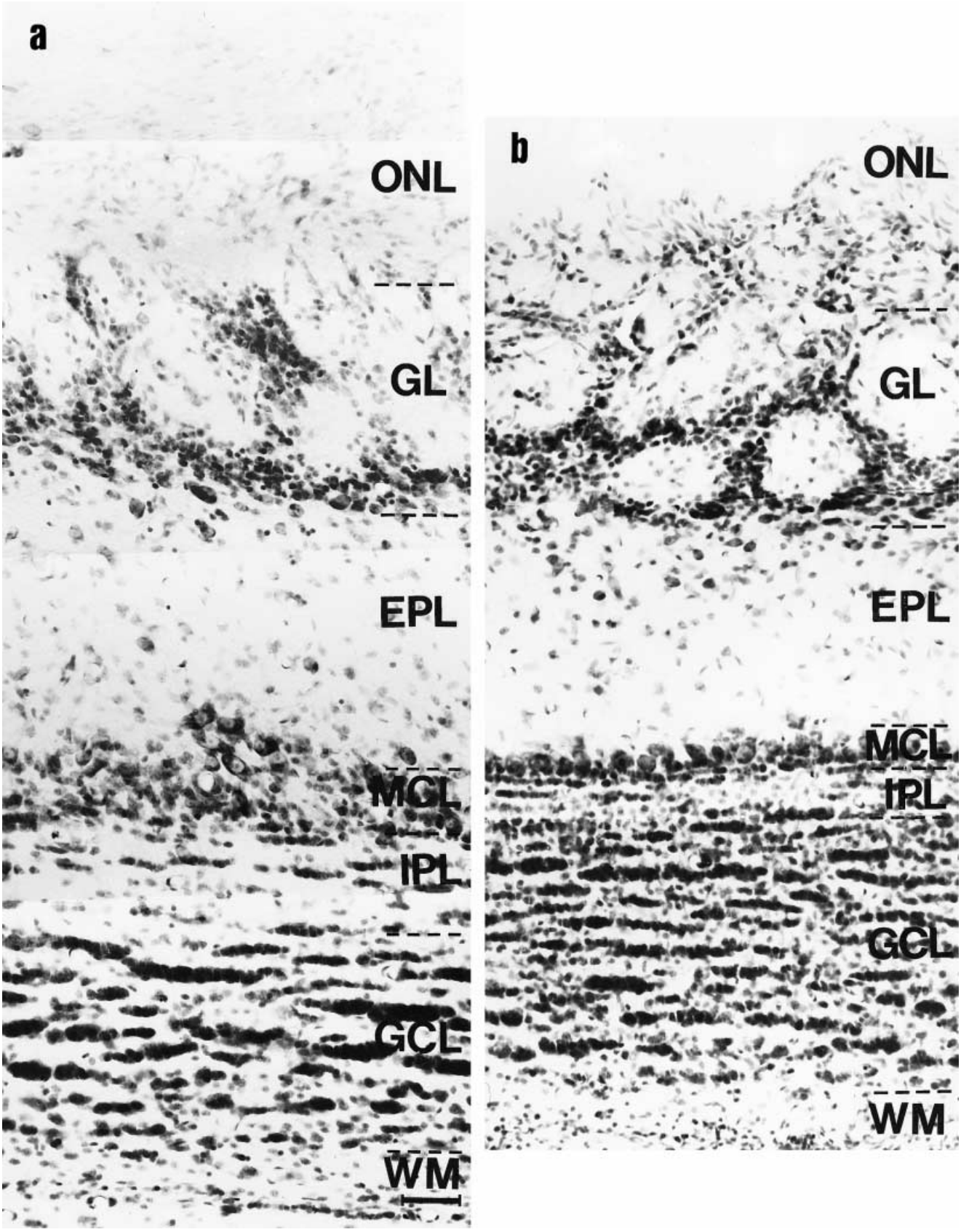

Fig. 2. Photographic composition of coronal Nissl-stained sections of the olfactory bulb in *Macaca fuscata* (**a**) and rat (**b**). Note the higher number of periglomerular cells in rat than in macaque, and the irregular arrangement of the mitral cells in the macaque rather than the monocellular mitral cell layer (MCL) of the rat. GCL, granule cell layer; GL, glomerular layer; EPL, external plexiform layer; IPL, internal plexiform layer; ONL, olfactory nerve layer; WM, white matter. Scale bar = 1 mm.

IPL, which is larger in the monkey. Clear differences are also observed in the number and density of different neuronal types. Periglomerular cells in the GL and granule cells in the GCL are more abundant, forming denser clusters in the rat in comparison with those in the monkey. Finally, in the macaque monkey the anterior olfactory nucleus has not a defined boundary. It penetrates into the olfactory bulb along with the WM, forming dispersed cellular masses immersed within the GCL of the olfactory bulb.

General characteristics of the ND and NOS staining

With the remarkable exception of the olfactory fibers, which were ND-positive but NOS-immunonegative, similar stained elements were found in the OB of the three species of macaque monkey after ND histochemistry or NOS immunohistochemistry. However, there were minor differences between both stainings. After the ND histochemical staining, strongly and weakly labeled cells were observed. These differences in the staining intensity were not so pronounced using NOS immunohistochemistry and thus, neuronal types that were faintly ND-stained were more clearly detected after NOS immunostaining. Besides, ND-stained elements demonstrated normally a more complete labeling of positive elements, including portions of the dendritic tree and lengthy axons that were not so clearly observed after NOS immunocytochemistry.

The ND and NOS staining patterns were consistent among all three species of macaque monkey, *Macaca fascicularis*, *Macaca fuscata*, and *Macaca nemestrina*. Neurons with similar morphological features and staining intensities were observed in the same zones of different species and animals, indicating that relatively stable populations of neurons exhibit ND and NOS reactivity. Thus, in our description we do not refer to individual species but to a general description of the labeled elements in the macaque monkey OB. The ND/NOS-active neurons showed different sizes, shapes, and dendritic branching patterns, indicating that they were a heterogeneous population including different neuronal types. Subpopulations of periglomerular cells and granule cells exhibited a weak ND/NOS staining. Other ND/NOS-positive elements were strongly stained, demonstrating well-defined dendrites and lengthy axons. They were easily identified as belonging to two of the previously defined neuronal types of the mammalian olfactory bulb, superficial short-axon cells, and deep short-axon cells. A population of medium-sized, weakly labeled neurons was observed in both the superficial and the deep layers of the macaque monkey OB. According to the size and shape of their neuronal bodies and the characteristics of their dendritic arborizations, these cells did not correspond to previously defined neuronal types observed by using other techniques such as silver impregnation or immunocytochemistry in either the rodent or the macaque OB. Thus, these cells were considered a new neuronal type characteristic of the macaque monkey OB and they were named superficial or deep stellate cells. Table 1 summarizes the distribution, size, and relative frequency of ND/NOS-labeled neurons within the *Macaca nemestrina* OB.

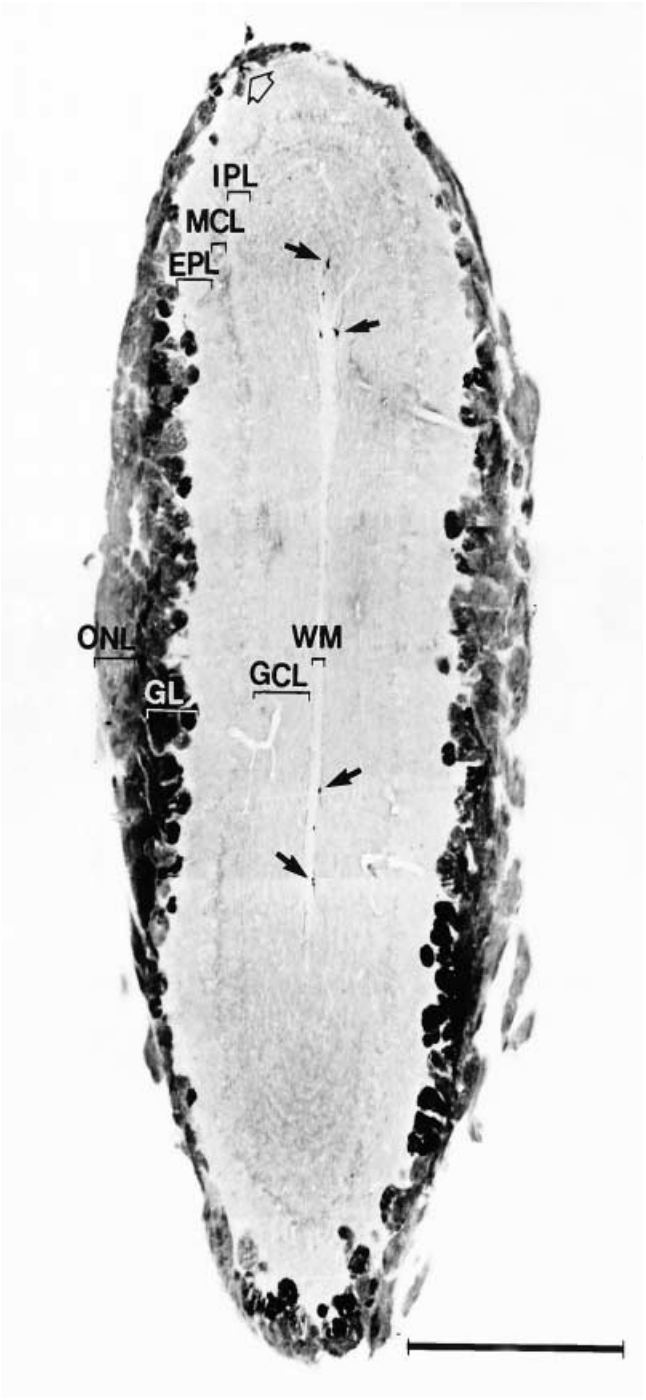

Fig. 3. Photographic composition of a coronal section of the olfactory bulb in the macaque monkey (*Macaca nemestrina*) after NADPH-diaphorase (ND) histochemical staining. Note the presence of ND activity in all olfactory fibers and glomeruli, and ND-positive somata in the GL/EPL boundary (open arrow) and GCL/WM boundary (arrows). GCL, granule cell layer; GL, glomerular layer; EPL, external plexiform layer; IPL, internal plexiform layer; MCL, mitral cell layer; ONL, olfactory nerve layer; WM, white matter. Scale bar = 1 mm.

ND and NOS: Somal and fiber localization

Under low magnification, all olfactory fibers were ND-active (Fig. 3). In the macaque monkey olfactory bulb, olfactory fibers extended throughout the periphery of the OB, including the dorsal side. Bundles of olfactory fibers could be followed through the GL and into a single

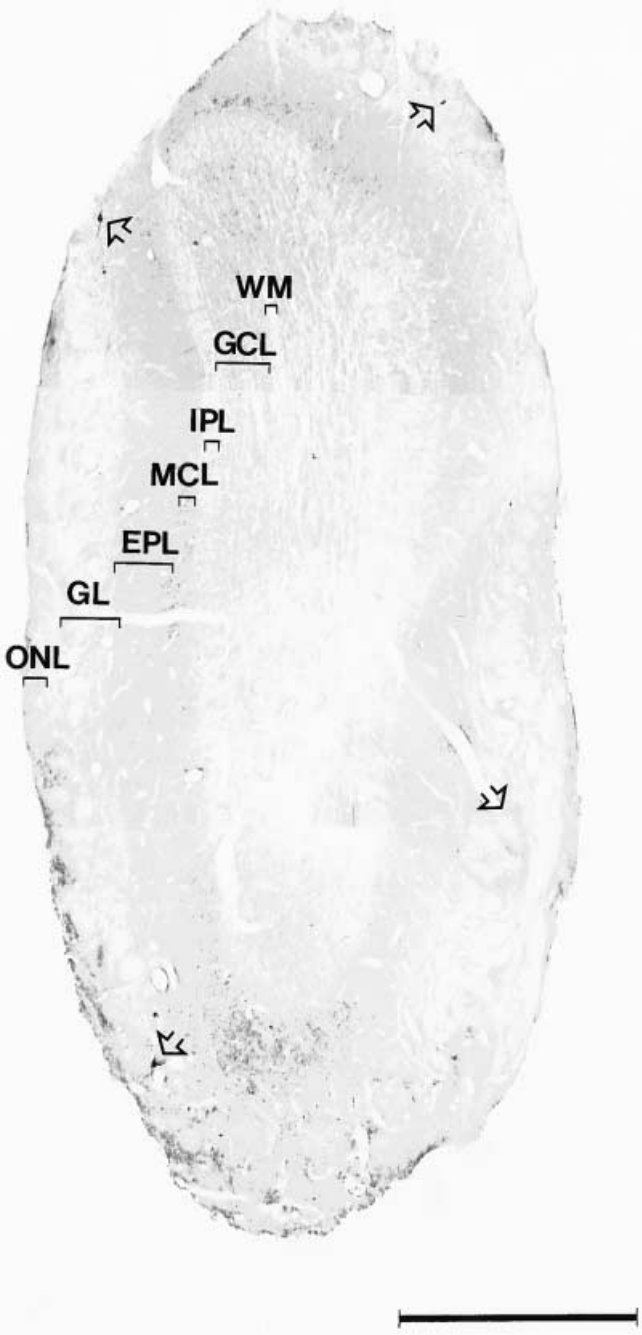

Fig. 4. Photographic composition of a coronal section of the *Macaca fuscata* olfactory bulb (OB) after neuronal nitric oxide synthase (NOS) immunohistochemistry. Immunoreactivity against NOS is absent in all olfactory fibers and glomeruli. Note the presence of NOS-immunopositive neurons in the GL (arrows). GCL, granule cell layer; GL, glomerular layer; EPL, external plexiform layer; IPL, internal plexiform layer; MCL, mitral cell layer; ONL, olfactory nerve layer; WM, white matter. Scale bar = 1 mm.

spherical or elliptical glomerulus (70–100 µm maximum diameter), terminating in a dense, circunscribed region of ND activity (Fig. 5a,b). All glomeruli demonstrated a heavy ND staining, although some differences in the labeling intensity were found. By contrast, NOS immunoreactivity was absent in olfactory fibers and glomeruli (Fig. 4).

The ND/NOS staining of intrinsic neuronal types of the OB was scarce. In the boundary between the GL and the EPL, a few ND/NOS-positive cells were observed. According to their size, morphology, and staining intensity, these cells were classified into three different neuronal types. The first population was formed by large cells (22–26 µm maximum diameter) demonstrating a strong ND/NOS staining (Figs. 5f, 7d). The cell nucleus could not be observed because of the dense cytoplasmic labeling. These ND/NOS-active neurons had round, fusiform, or oval somata with two to four long dendrites extending among the glomeruli. No dendrite from these cells could be traced within a glomerulus. These dendrites demonstrated a radial orientation in the sagittal sections, whereas in the coronal sections, they showed an oriented disposition, parallel to the olfactory bulb layers. The dendrites extended several hundred µm from the soma and they never passed into the deep portions of the EPL. They were densely covered with spines (Fig. 5g). Axon-like processes were observed arising from the soma or from a proximal dendrite and could be followed for long distances in the GL and EPL. These ND/NOS-active neurons were identified as superficial short-axon cells.

The second population was formed by weakly labeled cells also distributed in the GL/EPL boundary. These ND/NOS-active neurons had round cell bodies (12–18 µm maximum diameter) and the cell nucleus was clearly visible (Figs. 5d,e, 7c,d). Only the proximal dendrites and the axon initial segment were stained. Four or five dendritic trunks were radially oriented in both the sagittal and the coronal sections, and they did not demonstrate spines. The dendrites of these neurons did not enter apparently inside the glomeruli. Based upon these characteristics, we consider them a unique neuronal type for the macaque monkey OB. We have termed them as superficial stellate cells.

The third population is formed by ND/NOS-positive periglomerular cells (Figs. 5c, 7a–d). These cells were weakly labeled and had round or piriform small somata (9–10 µm of maximum diameter) which gave rise to stained intraglomerular dendrites. Most frequently a single dendrite entered within a single glomerulus, and more rarely, two primary dendrites arose from the somata and entered either a single or different adjacent glomeruli.

The only ND/NOS-labeled elements in the EPL, MCL, and IPL were scarce positive fibers coursing from deeper layers to the superficial layers. Most of these fibers were located in the EPL and had an orientation parallel to the olfactory bulb layers.

The most abundant ND/NOS-active cells were observed in the inner portion of the GCL and in the WM. As in the superficial strata, and according to their morphological and staining characteristics, three different ND/NOS-active neuronal populations were differentiated. The most conspicuous elements were large (21–39 µm) darkly stained cells (Figs. 6a–c, 8a). These ND/NOS-active neurons were located in the WM, and in lower number in the innermost portion of the GCL. They were identified as deep short-axon cells. These neurons included probably deep short-axon cells of the anterior olfactory nucleus that penetrates the OB along with the white matter, i.e., the rostral extension of the anterior commissure. They had variable morphologies including ovoid, pyramidal, bipolar, piri-

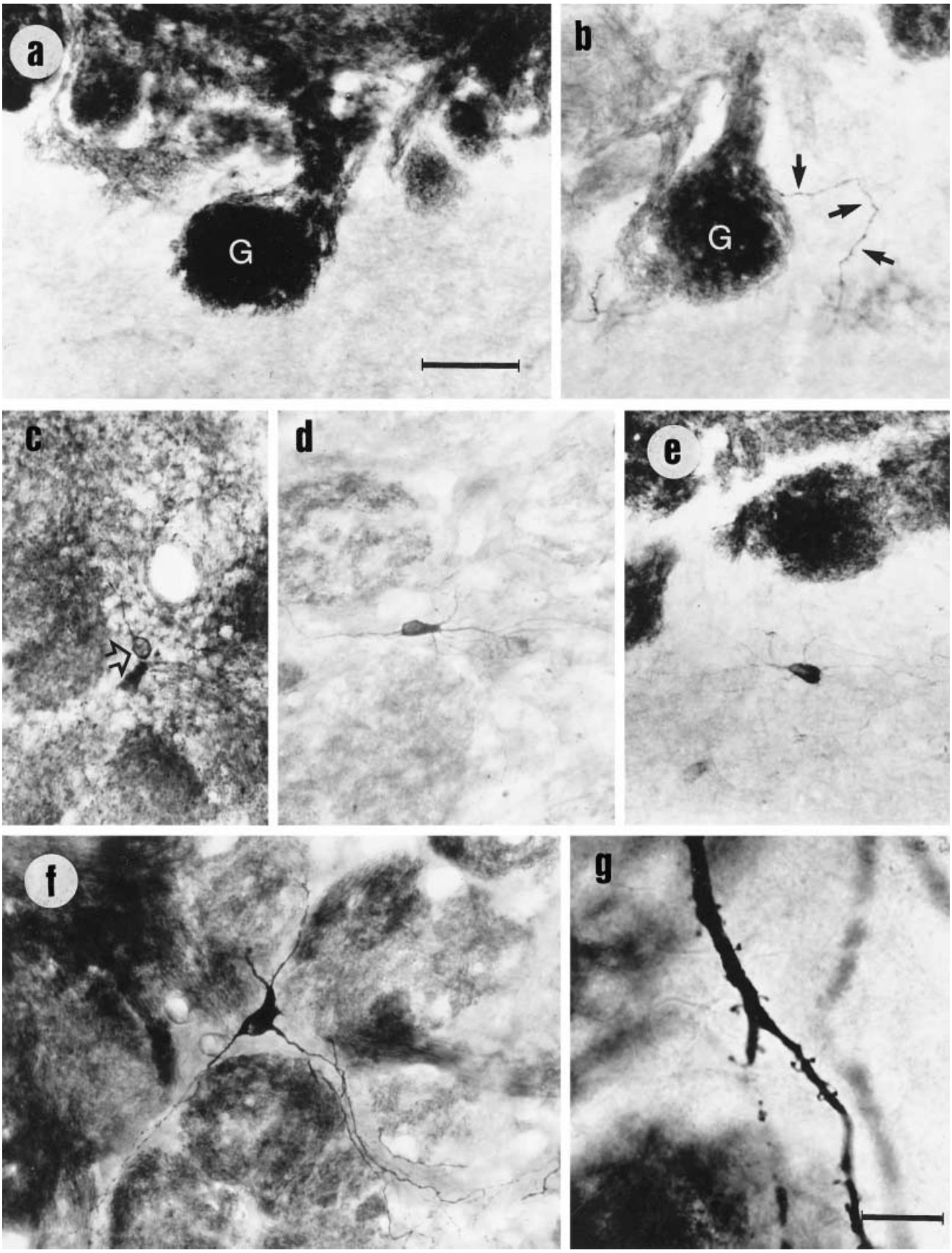

Figure 5

form, or triangular cell bodies, densely filled with formazan reaction product. Three to seven multipolar dendrites arose from each cell body and extended for several hundred µm. These cells were clearly oriented. In sagittal sections, the dendrites were oriented radially in all directions (Figs. 6a,c, 8a). In coronal sections, by contrast, the dendrites showed a parallel orientation to the OB layers. Altogether these cells had a characteristic "flattened" aspect (Fig. 6b). The dendrites were densely covered with spines (Figs. 6d, 8b), and branched one or two times in a wide dendritic field. The distal dendrites were clearly varicose. The axon could be followed in the WM and in the GCL, giving abundant collaterals that extended in the GCL and the anterior olfactory nucleus. In the caudal portion of the OB, close to the olfactory peduncle, fusiform cells with two primary dendrites (Fig. 8c) were especially abundant.

The second population of ND/NOS-active cells in the deep layers of the OB was formed by medium-sized (12–17 µm) and weakly positive neurons. These cells had round, ovoid, or piriform cell bodies in which the cell nucleus was clearly visible (Figs. 6f,g, 7f). Although they were relatively scarce, they were more abundant in the deep zone of the GCL and, more rarely, in the WM (Fig. 6b). Two to four primary dendrites were observed. These dendritic trunks were thin, weakly labeled and they could be followed only for a short distance. These ND/NOS-active cells did not correspond to previously defined neuronal types and, in order to be consistent with the nomenclature used for the weakly labeled neurons described in the GL/EPL boundary, we refer to them as deep stellate cells.

The third population of ND/NOS-stained cells in the deep layers was constituted by numerous granule cells (Figs. 6e, 7e,f, 8a–c). These cells were small (7–8 µm of maximum diameter), with round or oval shapes. They were weakly labeled; only a thin rim of cytoplasm surrounding the negative cell nucleus was observed. Only a subpopulation of granule cells was ND/NOS-positive, and they were more abundant in the innermost portion of the GCL, with some ND/NOS-active granule cells displaced within the WM.

In addition to these three populations of ND/NOS-active neurons, labeled fibers were observed in the GCL and WM. Most of these fibers were thick, intensely stained, varicose, and they coursed parallel to the OB lamination (Fig. 6g). Many of them could be followed from the olfactory tract, reaching the dorsal and ventral regions of the WM, and being identified as centrifugal fibers. Most centrifugal fibers remain in the WM or inner GCL but a reduced group could be followed through the outer GCL and among the negative profiles of the mitral cells, reaching the EPL, and even the GL (Fig. 5b). The axons of the ND/NOS-stained deep short-axon cells intermingled with the centrifugal fibers but they were easily distinguished due to their thinner diameter and more restricted distribution.

In summary, ND/NOS activity in the macaque monkey olfactory bulb was detected in extrinsic afferent fibers and intrinsic neuronal types. Extrinsic fibers included ND-stained olfactory fibers (all of them) and a restricted subpopulation of ND/NOS-labeled centrifugal fibers from higher brain areas. ND/NOS-active intrinsic cells were typified as interneurons located in both superficial layers (periglomerular cells, superficial short-axon cells, and superficial stellate cells) and deep layers (granule cells, deep short-axon cells, and deep stellate cells); (Fig. 9).

DISCUSSION

This paper provides a comprehensive description of the distribution and morphological characteristics of ND/NOS-active neurons and fibers in the macaque monkey OB.

Interspecies differences in the ND/NOS staining

Comparing our results in the macaque monkey with the distribution of ND/NOS somal staining in the OB of other mammals, both differences and similarities are present. The main similarity between macrosmatic and microsmatic animals is the presence of ND/NOS staining in intrinsic interneurons and olfactory and centrifugal afferent fibers. The differences include the characterization of ND/NOS-positive neuronal types and the absence in primates of ND-negative olfactory fibers. Concerning the somal staining, ND/NOS-labeled superficial short-axon cells have been observed in all rodents hitherto studied (rat: Scott et al., 1987; Croul-Ottman and Brunjes, 1988; Villalba et al., 1988, 1989; Davis, 1991; Vincent and Kimura, 1992; Alonso et al., 1993; Hopkins et al., 1996; Briñón et al., 1997; mouse: Kishimoto et al., 1993; hamster: Davis, 1991), and in the three species of macaque monkeys, but not in the hedgehog (Alonso et al., 1995b). In rodents and insectivores, horizontal cells and many periglomerular cells were ND/NOS-active (Scott et al., 1987; Villalba et al., 1988, 1989; Davis, 1991; Vincent and Kimura, 1992; Alonso et al., 1993, 1995b; Briñón et al., 1997), whereas no horizontal cells and only a few periglomerular cells were ND/NOS-positive in the macaque monkey OB. Because of this fact, most somal staining was not located in the GL as in rodents (Davis, 1991) but in the GCL/WM boundary. The existence of darkly stained deep short-axon cells, superficial and deep weakly labeled neurons, as well as stained granule cells is coincident with previous observations in rodents (Davis, 1991; Vincent and Kimura, 1992; Briñón et al., 1997), although there are some differences in their morphological characteristics.

Major interspecies differences were also observed in the ND fiber staining. Contrary to what has been reported in macrosmatic animals, in which only a spatially segregated subpopulation of olfactory fibers and glomeruli demonstrated ND staining (Scott et al., 1987; Croul-Ottman and Brunjes, 1988; Davis, 1991; Vincent and Kimura, 1992; Kishimoto et al., 1993; Alonso et al., 1993, 1995b; Hopkins et al., 1996), all olfactory fibers and glomeruli were ND-active in the three species of macaque monkeys, *Macaca fascicularis, Macaca fuscata,* and *Macaca nemestrina*. The distribution and morphological characteristics of centrifu-

Fig. 5. NADPH-diaphorase (ND) activity in the superficial layers of the olfactory bulb *Macaca nemestrina* (a,c,d,f,g) and *Macaca fascicularis* (b,e). **a:** Intense ND staining in the olfactory fibers. A dense fascicle of fibers arborizing in a glomerulus (G) can be observed. **b:** ND-positive centrifugal fiber (arrows) reaching the glomerular layer. **c:** ND-positive monodendritic periglomerular cell (arrow). **d,e:** ND-positive superficial stellate cells in the glomerular layer (GL)/external plexiform layer (EPL) boundary. d, sagittal view; e, coronal view. **f:** ND-active superficial short-axon cell in a sagittal section. Note the course of the dendrites in the periglomerular region, without entering within the glomeruli. **g:** Higher magnification of one dendrite of the neuron showed in f. Pedunculated spines can be clearly observed. Scale bars = 50 µm in a–f, 10 µm in g.

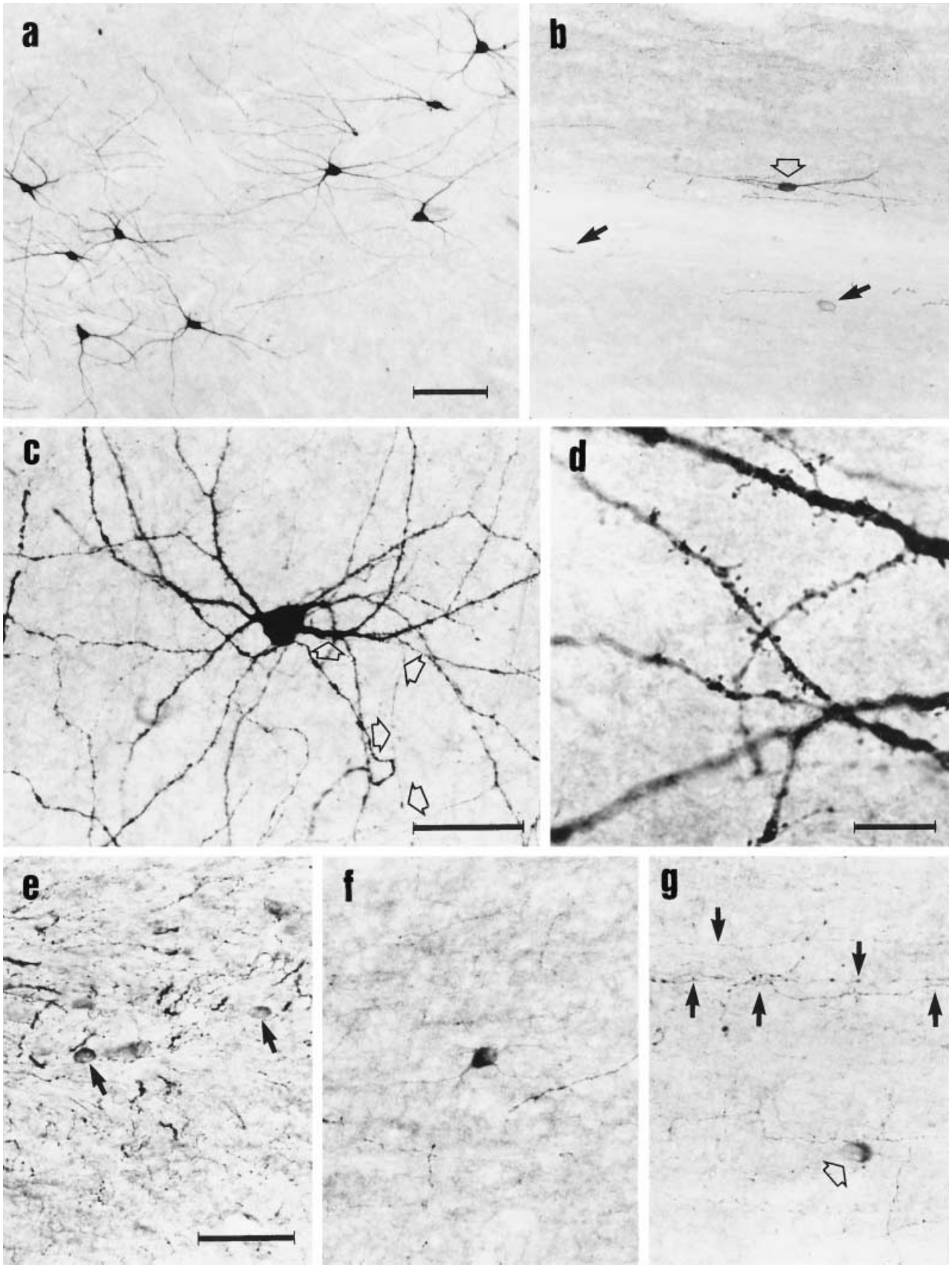

Fig. 6. NADPH-diaphorase (ND)-active neurons in the deep layers of the olfactory bulb. *Macaca nemestrina* (a,b,e,f,) and *Macaca fascicularis* (c,d,g). **a:** ND-active deep short-axon cells in the white matter. Sagittal section. **b:** An oriented deep short-axon cell (open arrow) and two deep stellate cells (arrows) can be observed close to the granule cell layer (GCL)/white matter (WM) boundary. Coronal section. **c:** ND-active deep short-axon cell. The axon arising from a proximal dendrite can be followed (open arrows). **d:** Detail of the dendrites of a deep short-axon cell. Abundant dendritic spines can be observed. **e:** ND-positive granule cells (arrows) among ND-stained centrifugal fibers in the GCL/WM boundary. **f:** ND-active deep stellate cell located in the GCL. Weakly stained dendrites can be noted. Sagittal section. **g:** Coronal section through the GCL/WM boundary. Abundant oriented varicose fibers (arrows) and a deep stellate cell body (open arrow) can be observed. Scale bars = 50 µm in a–c and e–g, 10 µm in d.

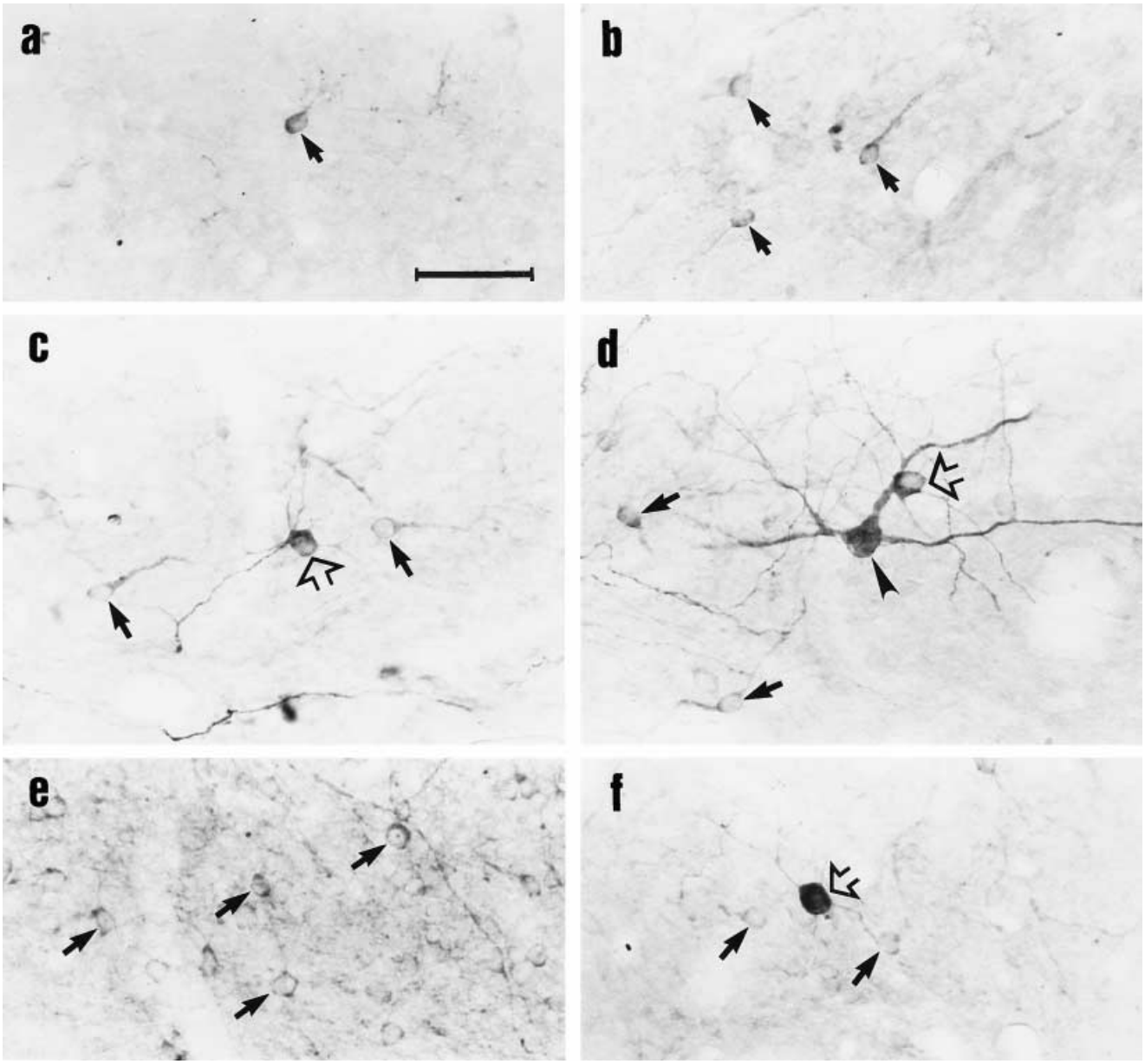

Fig. 7. Neuronal nitric oxide synthase (NOS)-immunoreactive neurons in coronal sections of the olfactory bulb. *Macaca fuscata* (a,c,d,f,) and *Macaca fascicularis* (b,e). **a,b:** NOS-immunoreactive periglomerular neurons (arrows) showing diverse orientations and branching patterns of the dendritic tree. **c:** NOS-immunopositive superficial stellate cell (open arrow) and periglomerular cells (arrows) in the glomerular layer (GL)/ external plexiform layer (EPL) boundary. **d:** NOS immunoreactivity in the GL/EPL boundary. A superficial short-axon cell (arrowhead), a superficial stellate cell (open arrow), and two periglomerular cells (arrows) show different staining intensities.**e:** Weakly NOS-immunoreactive granule cells (arrows) in the granule cell layer (GCL). **f:** NOS-immunoreactive deep stellate cell (open arrow) located in the GCL. Weakly stained granule cells (arrows) can be noted. Scale bar = 50 μm.

gal fibers is similar in the macaque monkey OB to previous reports in rodents (Davis, 1991), although the dense ND-active neuropile described surrounding the granule cells (Davis, 1991) is not present in our preparations.

Our data indicate that complexity of ND/NOS staining in the OB corresponds to the level of development of the olfactory sense. Thus, the ND/NOS-labeled neurons in the macaque monkey OB were less abundant and showed a lower morphological diversity than the staining described in rodents (rats and mice; Davis, 1991; Vincent and Kimura, 1992; Alonso et al., 1993; Hopkins et al., 1996). Similarly, rodents have simpler ND/NOS staining patterns than the hedgehog, an insectivorous with extraordinarily developed olfactory structures (Alonso et al., 1995b). Stephan and Andy (1970) have shown that the OB accounts for 17.6% of the volume of the telencephalon in the hedgehog, whereas this ratio is reduced to 2.9% in prosimians and 0.2% in simians. Allometric studies demonstrate that the size of OB does diminish in correlation to the decrease in the functional significance of the olfactory

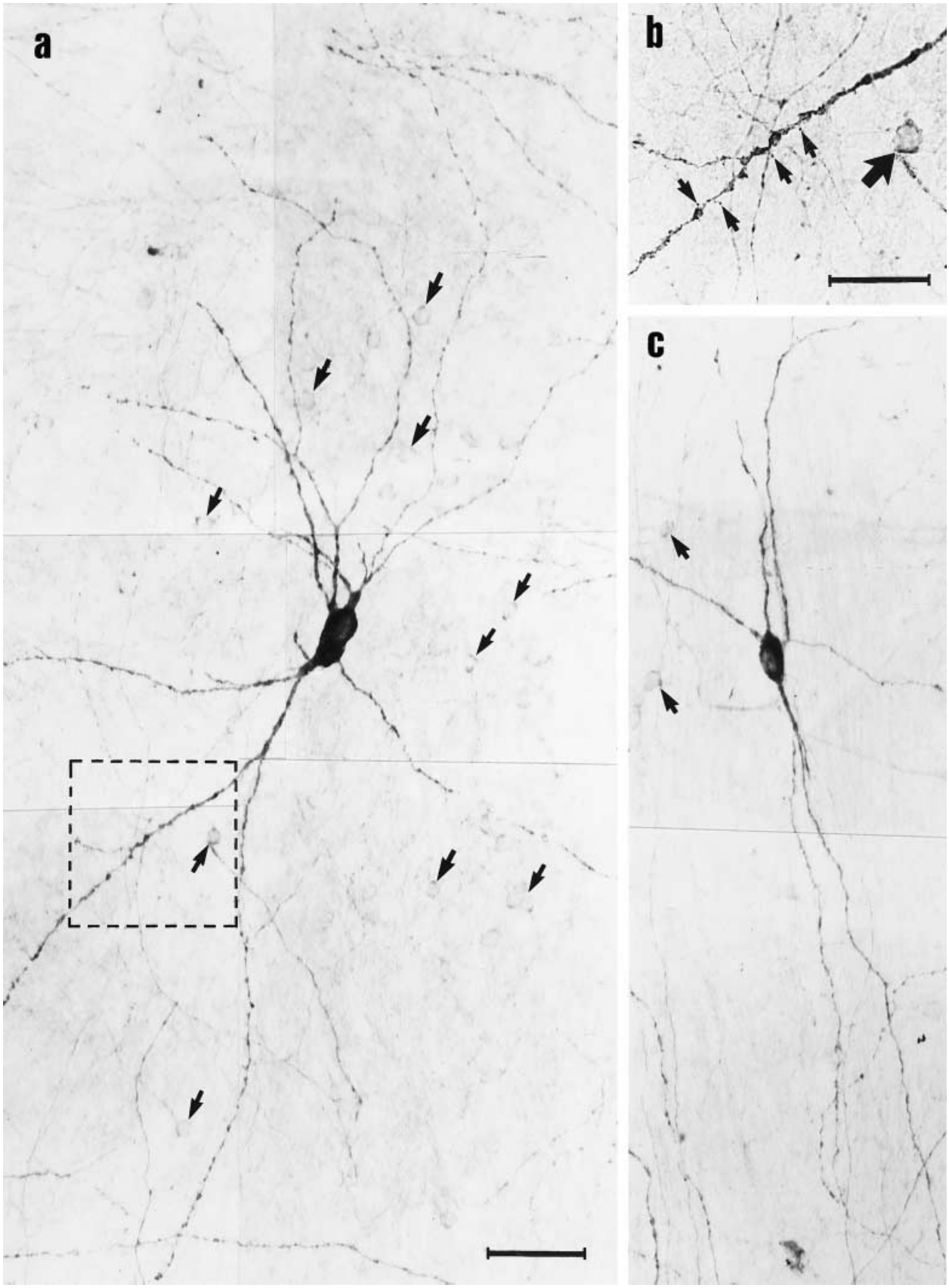

Fig. 8. Neuronal nitric oxide synthase (NOS)-immunoreactive neurons in sagittal sections of the olfactory bulb. *Macaca fuscata* (a,b) and *Macaca nemestrina* (c). **a:** Photographic composition of the granule cell layer (GCL). A large and strongly NOS-immunoreactive deep short-axon cell is accompanied by small and slightly NOS-immunostained granule cells (arrows). **b:** Magnification of the area squared in a, showing in detail the dendritic spines (small arrows) of a deep short-axon cell, and the localization of NOS immunoreaction in a thin cytoplasmic rim surrounding the negative nucleus of a granule cell (large arrow). **c:** Bipolar NOS-immunoreactive deep short-axon cell located in the white matter (WM) of the initial portion of the olfactory peduncle. Displaced NOS-immunostained granule cells are also observed (arrows). Scale bars = 50 µm in a,c, 20 µm in b.

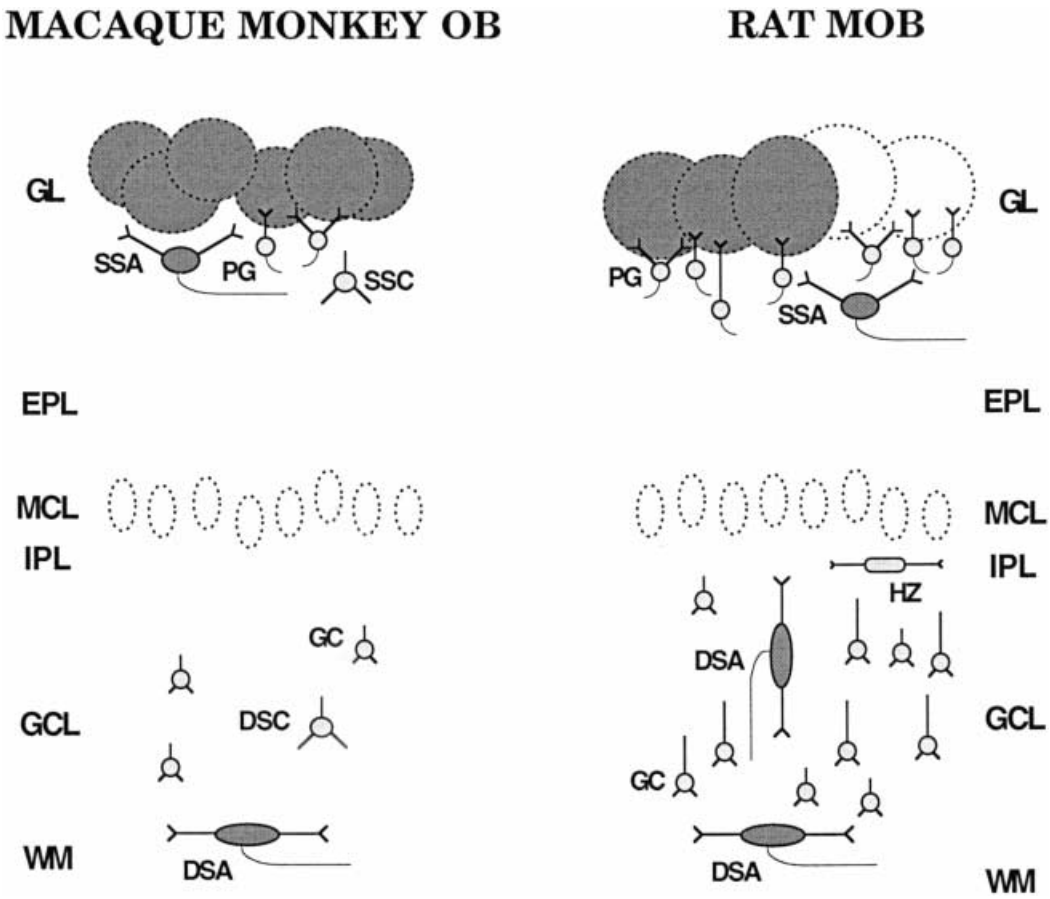

Fig. 9. Schematic drawing showing the differential NADPH-diaphorase (ND) staining patterns in the olfactory bulb (OB) of the macaque monkey and the rat. DSA, deep short-axon cell; DSC, deep stellate cell; EPL, external plexiform layer; GC, granule cell; GCL, granule cell layer; GL, glomerular layer; HZ, horizontal cell; IPL, internal plexiform layer; MCL, mitral cell layer; MOB, main olfactory bulb; OB, olfactory bulb; PG, periglomerular cell; SSA, superficial short-axon cell; SSC, superficial stellate cell; WM, white matter.

system. We conclude that the differences in the ND/NOS labeling seem to correlate with the relative volume of the OB, and with the functional significance of olfaction in the biology of the species. Studies in other groups of vertebrates seem to confirm this hypothesis; thus, no ND staining is observed in the secondarily simplified OB of birds (Panzica et al., 1994), and only olfactory fibers are ND-positive in the OB of teleosts (Arévalo et al., 1995).

Identification of ND/NOS-active elements in the macaque monkey OB

ND activity has been observed in olfactory receptor cells in the human olfactory mucosa (Kulkarni et al., 1994). Although these same authors reported that olfactory nerve bundles were unstained, our group has found that human olfactory fibers and glomeruli demonstrated ND staining (Briñón et al., 1998). We consider that this discrepancy can be due to differences in the fixation, incubation procedure, or to postmortem delay. Thus, it appears that ND activity in all olfactory fibers is a common characteristic of both human and nonhuman primates.

The ND/NOS-stained cells of the GL and GL/EPL boundary were identified as superficial short-axon cells and periglomerular cells. The morphology of these neurons is consistent with previous descriptions of this neuronal type using silver impregnation (Pinching and Powell, 1971; Schneider and Macrides, 1978) and calcium-binding proteins, dopamine, neuropeptide Y, somatostatin, cholecystokinin, tyrosine hydroxylase, vasoactive intestinal polypeptide, and γ-aminobutyric acid immunocytochemistry (see Halász, 1990, for a review), and ND histochemistry (Scott et al., 1987; Vincent and Kimura, 1992; Alonso et al., 1993, 1995b; Hopkins et al., 1996; Briñón et al., 1997).

In rat and hamster EPL, weakly ND-labeled neurons were also observed. These cells could be identified as small middle tufted cells because they are oriented and possess an intraglomerular dendrite (Davis, 1991). However, these characteristics could not be distinguished in the weakly labeled neurons described in the monkey EPL. Weakly labeled neurons in the GCL, with similar size to our deep stellate cells, have been also reported in rodents after ND-histochemistry (Vincent and Kimura, 1992) but they have not been characterized.

Granule cells are the most numerous interneurons in the vertebrate olfactory bulb. The subpopulation of ND/NOS-stained granule cells of the macaque monkey OB displays similar morphology and size as the ND/NOS-positive granule cells in the rodent and insectivorous OB (Davis, 1991; Alonso et al., 1993, 1995b; Hopkins et al., 1996). Also consistent with observations in the rat (Scott et

al., 1987; Davis, 1991; Vincent and Kimura, 1992; Hopkins et al., 1996), we have identified the darkly stained cells of the GCL and WM in the monkey as deep short-axon cells. The morphology of these cells is generally similar to those of deep short-axon cells impregnated with the Golgi method (Ramón y Cajal, 1904; Price and Powell, 1970; Schneider and Macrides, 1978) or neuropeptide Y immunohistochemistry (Scott et al., 1987; Gall et al., 1986) in the OB of macrosmatic mammals. However, the cells identified in the primate exhibit unique characteristics. The ND/NOS-stained deep cells of the macaque monkey are larger (21–39 μm maximum diameter) than similar cells described in rodents (17–18 μm maximum diameter; Scott et al., 1987; Davis, 1991). In addition, Scott et al. (1987) did not observe spines on these cells or their dendrites, whereas they were clearly spiny in our preparations. It is uncertain to ascribe the ND/NOS-labeled deep short-axon cells to one of the several classes of deep short-axon cells described in the literature. The ND/NOS-stained deep short-axon cells may correspond to Blanes cells because they are described as spiny neurons in agreement with our observations in the macaque monkey OB. However, Blanes cells are described as unoriented cells (Schneider and Macrides, 1978), whereas the cells in the monkey OB were clearly oriented. The larger size of the macaque monkey cells, their location in the deep GCL and in the WM, and their oriented dendrites parallel to the OB lamination resemble the giant cells, described with calbindin D-28k immunohistochemistry (Briñón et al., 1992). However, rat giant cells do not possess spines, their proximal dendrites are varicose, and they have not been observed after ND/NOS staining in the rat OB.

In rodents, there is evidence suggesting that the number of neurons belonging to a neuronal type is much higher than the subclass identified after ND/NOS staining. Although the cytoarchitecture of the macaque OB has not been as extensively studied, the low number of ND/NOS-active elements and their distribution strongly suggest that, as is the case in other OB neuronal types (Alonso et al., 1993), ND/NOS-active neurons in the macaque monkey OB constitute a subpopulation of the same morphological neuronal types.

Functional implications

It has been demonstrated that the olfactory fibers of mouse (Kishimoto et al., 1993), rat (Kulkarni et al., 1994; Spessert et al., 1994), and human (Kulkarni et al., 1994; Briñón et al., 1998) do not contain NOS, although they display a strong ND labeling. The enzyme responsible for this staining has been presumably identified as cytochrome P450 reductase, an enzyme that shares certain molecular features with NOS (Bredt et al., 1991b; Lowenstein and Snyder, 1992). In contrast, all ND-positive neurons in the OB also exhibited NOS immunoreactivity and all the investigated NOS-positive neurons exhibited ND activity (Spessert et al., 1994; Hopkins et al., 1996). The presence of ND-positive staining in all olfactory fibers and glomeruli in the macaque monkey OB is not only an important interspecies difference but an argument against some of the hypotheses proposed to explain the clear-cut distribution pattern of ND-active fibers in the rodent OB. Whereas in rodents the olfactory receptor cells are either ND-positive or ND-negative and project to definite and segregated targets identified as a ND-positive or ND-negative glomerulus, respectively, this topographical segregation is not present in the macaque monkey OB. Kishimoto et al. (1993) have suggested that the topographical distribution of ND-positive and ND-negative glomeruli may reflect specific odor stimulation and neuronal activity. Indeed, it has been demonstrated that a given odor activates a set of olfactory receptor cells that has input to a spatially defined set of glomeruli within the OB (Stewart et al., 1979; Jastreboff et al., 1984). Mori et al. (1992) have shown that mitral cells in the dorsomedial region of the rabbit OB, the same region where in rodents and insectivores are located the ND-positive glomeruli, respond differentially to fatty acids. Immunohistochemical studies have shown that different subsets of glomeruli are antigenically distinct. The distribution patterns of some antigens are relatively similar (e.g., 2B8 against membrane surface glycoproteins, and CC2 against carbohydrates) or complementary (e.g., R4B12) to the ND-active glomeruli of the rat OB (Allen and Akeson, 1985; Fujita et al., 1985; Mori et al., 1985; Mori, 1987). Some lectins such as soybean agglutinin, *Ulex europaeus* 1, and *Lotus tetragonolobus* also demonstrate differential labeling patterns in the adult rat OB (Scott et al., 1993). Because the ND staining pattern in the macaque monkey glomeruli is a homogenous heavy staining, it would be interesting to know whether the staining pattern for these antigens and lectins is segregated in the macaque monkey OB.

Breer and Shepherd (1993) have suggested that nitric oxide alters within the glomerulus the neuronal response to odorant stimulation in the olfactory receptors. Previous hypotheses proposing a major role for nitric oxide in the signal transduction mechanism in the olfactory system (Vincent and Kimura, 1992) could be sustained despite the absence of NOS in olfactory fibers because all glomeruli were surrounded by abundant ND/NOS-positive periglomerular cells. The same role for nitric oxide could exist in the macaque monkey OB, but its significance in the olfactory modulation seems to be lower than in macrosmatic mammals because numerous glomeruli are not surrounded by any ND/NOS-positive neuron, and in those which posses ND/NOS-positive juxtaglomerular neurons, the number is clearly lower in the macaque monkey than in rodents or insectivores.

ND-active neurons are selectively spared in clinical neurodegenerative disorders, such as Huntington's and Alzheimer's diseases (Ferrante et al., 1985; Hyman et al., 1992) as well as following hypoxic or neurotoxic damage of the brain (Koh et al., 1986; Uemura et al., 1990). The olfactory system is the sensory system that is more severely affected in Alzheimer's disease (Ohm and Braak, 1987; Talamo et al., 1991). The anatomical substrate is not known, but olfactory discrimination and sensitivity are also affected early in the clinical course of the disease (Serby et al., 1985; Doty et al., 1987). The production of nitric oxide by restricted neuronal populations, those identified after ND histochemistry and NOS immunohistochemistry, has been considered a possible main factor in the characteristic neuronal death and neuronal survival present in Huntington's or Alzheimer's diseases. It has been suggested that nitric oxide mediates N-methyl-D-aspartate receptor-linked excitotoxicity, and that neurons containing NOS are themselves spared from nitric oxide toxic effects (Dawson et al., 1991). The OB appears to provide an excellent model system in which to investigate the physiological meaning of ND/NOS activity and the factors that alter its distribution pattern. Finally, our

comparative data indicate that experimental models based on rodents do not provide an accurate estimation of the distribution pattern of ND/NOS-positive elements in the primate olfactory system, in order to check the effect of different conditions on ND/NOS activity.

ACKNOWLEDGMENTS

The authors express their gratitude to Dr. C. Cavada, Dr. E. Rausell, and Dr. D.G. Amaral for kindly providing some of the macaque monkey olfactory bulbs used in this study, Dr. Emson and Dr. Charles for kindly providing the anti-NOS K205 antiserum, and Dr. W. Suzuki for her comments on the manuscript.

LITERATURE CITED

Allen, W.K. and R. Akeson (1985) Identification of a cell surface glycoprotein family of olfactory receptor neurons with a monoclonal antibody. J. Neurosci. *5:*284–296.

Allison, A.C. (1953) The morphology of the olfactory system in the vertebrates. Biol. Rev. *28:*195–244.

Alonso, J.R., R. Arévalo, A. Porteros, J.G. Briñón, J. Lara, and J. Aijón (1993) Calbindin D-28K and NADPH-diaphorase activity are localized in different populations of periglomerular cells in the rat olfactory bulb. J. Chem. Neuroanat. *6:*1–6.

Alonso, J.R., R. Arévalo, J.G. Briñón, E. García-Ojeda, A. Porteros, and J. Aijón (1995a) NADPH-diaphorase staining in the central nervous system. Neurosci. Prot. *050–04:*1–11.

Alonso, J.R., R. Arévalo, E. García-Ojeda, A. Porteros, J.G. Briñón, and J. Aijón (1995b) NADPH-diaphorase active and calbindin D-28k-immunoreactive neurons and fibers in the olfactory bulb of the hedgehog (*Erinaceus europaeus*). J. Comp. Neurol. *351:*307–327.

Arévalo, R., J.R. Alonso, E. García-Ojeda, J.G. Briñón, C. Crespo, and J. Aijón (1995) NADPH-diaphorase in the central nervous system of the tench (*Tinca tinca* L., 1758). J. Comp. Neurol. *352:*398–420.

Baker, H. (1986) Species differences in the distribution of substance P and tyrosine hydroxylase immunoreactivity in the olfactory bulb. J. Comp. Neurol. *252:*206–226.

Baker, H., C. Abate, A. Szabo, and T.H. Joh (1991) Species-specific distribution of aromatic L-amino acid decarboxylase in the rodent adrenal gland, cerebellum, and olfactory bulb. J. Comp. Neurol. *305:* 119–129.

Bassett, J.L., M.T. Shipley, and S.L. Foote (1992) Localization of corticotropin-releasing factor-like immunoreactivity in monkey olfactory bulb and secondary olfactory areas. J. Comp. Neurol. *316:*348–362.

Bredt, D.S., C.E. Glatt, P.M. Hwang, M. Fotuhi, T.M. Dawson, and S.H. Snyder (1991a) Nitric oxide synthase protein and mRNA are discretely localized in neuronal populations of the mammalian CNS together with NADPH diaphorase. Neuron *7:*615–624.

Bredt, D.S., P.M. Hwang, C.E. Glatt, C. Lowenstein, R.R. Reed, and S.H. Snyder (1991b) Cloned and expressed nitric oxide synthase structurally resembles cytochrome P-450 reductase. Nature *351:*714–718.

Breer, H. and G. Shepherd (1993) Implications of the NO/cGMP system for olfaction. Trends Neurosci. *16:*5–9.

Briñón, J.G., J.R. Alonso, R. Arévalo, E. García-Ojeda, J. Lara, and J. Aijón (1992) Calbindin D-28k-positive neurons in the rat olfactory bulb. Cell Tissue Res. *269:*289–297.

Briñón, J.G., J.R. Alonso, E. García-Ojeda, C. Crespo, R. Arévalo, and J. Aijón (1997) Calretinin- and parvalbumin-immunoreactive neurons in the rat main olfactory bulb do not express NADPH-diaphorase activity. J. Chem. Neuroanat. *13:*253–264.

Briñón, J.G., C. Crespo, E. Weruaga, J. Alonso, T. Sobreviela, J. Aijón, and J.R. Alonso (1998) NADPH-diaphorase/nitric oxide synthase-positive elements in the human olfactory bulb. Neuroreport 9:3141–3146.

Croul-Ottman, C.E. and P.C. Brunjes (1988) NADPH-diaphorase within the developing olfactory bulbs of normal and unilaterally odor-deprived rats. Brain Res. *460:*323–328.

Davis, B.J. (1991) NADPH-diaphorase activity in the olfactory system of the hamster and rat. J. Comp. Neurol. *314:*493–511.

Dawson, T.M., D.S. Bredt, M. Fotuhi, P.M. Hwang, and S.H. Snyder (1991) Nitric oxide synthase and neuronal NADPH-diaphorase are identical in brain and peripheral tissues. Proc. Natl. Acad. Sci. USA *88:*7797–7801.

Doty, R.L., P.F. Reyes, and T. Gregor (1987) Presence of both odor identification and detection deficits in Alzheimer's disease. Brain Res. Bull. *18:*597–600.

Ferrante, R.J., N.W. Kowall, M.F. Beal, E.P. Richardson Jr., E.D. Bird, and J.B. Martin (1985) Selective sparing of a class of striatal neurons in Huntington's disease. Science *230:*561–563.

Fujita, S.C., K. Mori, K. Imamura, and K. Obata (1985) Subclasses of olfactory receptor cells and their segregated central projections demonstrated by a monoclonal antibody. Brain Res. *326:*192–196.

Gall, C., K.B. Seroogy, and N. Brecha (1986) Distribution of VIP- and NPY-like immunoreactivities in rat main olfactory bulb. Brain Res. *374:*389–394.

Halász, N. (1990) The Vertebrate Olfactory System. Chemical Neuroanatomy, Function and Development. Budapest: Akadémiai Kiadó.

Herbison, A.E., S.X. Simonian, P.J. Norris, and P.C. Emson (1996) Relationship of neuronal nitric oxide synthase immunoreactivity to GnRH neurons in the ovariectomized and intact female rat. J. Neuroendocrinol. *8:*73–82.

Hope, B.T., G.J. Michael, K.M. Knigge, and S.R. Vincent (1991) Neuronal NADPH-diaphorase is a nitric oxide synthase. Proc. Natl. Acad. Sci. USA *88:*2811–2814.

Hopkins, D.A., H.W.M. Steinbusch, M. Markerink-Van Ittersum, and J. De Vente (1996) Nitric oxide synthase, cGMP, and NO-mediated cGMP production in the olfactory bulb of the rat. J. Comp. Neurol. *375:*641–658.

Hyman, B.T., K. Marzloff, J.J. Wenninger, T.M. Dawson, D.S. Bredt, and S.H. Snyder (1992) Relative sparing of nitric oxide synthase-containing neurons in the hippocampal formation in Alzheimer's disease. Ann. Neurol. *32:*818–820.

Jastreboff, P.B., P.E. Pedersen, C.A. Greer, W.B. Stewart, J.S. Kauer, and G.M. Shepherd (1984) Specific olfactory receptor populations projecting to identified glomeruli in the rat olfactory bulb. Proc. Natl. Acad. Sci. USA *81:*5250–5254.

Kiernan, J.A. (1990) Histological and Histochemical Methods. Theory and Practice. Oxford: Pergamon Press.

Kishimoto, J., E.B. Keverne, J. Hardwick, and P.C. Emson (1993) Localization of nitric oxide synthase in the mouse olfactory and vomeronasal system: A histochemical, immunological and *in situ* hybridization study. Eur. J. Neurosci. *5:*1684–1694.

Koh, J.Y., S. Peters, and D.W. Choi (1986) Neurons containing NADPH-diaphorase are selectively resistant to quinolinate toxicity. Science *234:*73–76.

Kulkarni, A.P., T.V. Getchell, and M.L. Getchell (1994) Neuronal nitric oxide synthase is localized in extrinsic nerves regulating perireceptor processes in the chemosensory nasal mucosae of rats and humans. J. Comp. Neurol. *345:*125–138.

Lowenstein, C.J. and S.H. Snyder (1992) Nitric oxide, a novel biologic messenger. Cell *70:*705–707.

Matsutani, S., E. Senba, and M. Tohyama (1989) Distribution of neuropeptide-like immunoreactivities in the guinea pig olfactory bulb. J. Comp. Neurol. *280:*577–586.

Mestre, N., A. Petter, and N. Bons (1992) Systematisation of the olfactory bulb efferent projections in a lemurian primate: *Microcebus murinus.* J. Hirnforsch. *33:*173–184.

Mizukawa, K., S.T. Vincent, P.L. McGeer, and E.G. McGeer (1989) Distribution of reduced nicotine-adenine-dinucleotide-phosphate-diaphorase-positive cells and fibers in the cat central nervous system. J. Comp. Neurol. *279:*281–311.

Mori, K. (1987) Monoclonal antibodies (2C5 and 4C9) against lactoseries carbohydrates identify subsets of olfactory and vomeronasal receptor cells and their axons in the rabbit. Brain Res. *408:*215–221.

Mori, K., S.C. Fujita, K. Imamura, and K. Obata (1985) Immunohistochemical study of subclasses of olfactory nerve fibers and their projections to the olfactory bulb in the rabbit. J. Comp. Neurol. *242:*214–229.

Mori, K., N. Mataga, and K. Imamura (1992) Differential specificities of single mitral cells in rabbit olfactory bulb for a homologous series of fatty acid odor molecules. J. Neurophysiol. *67:*786–789.

Ohm, T.G. and H. Braak (1987) Olfactory bulb changes in Alzheimer's disease. Acta Neuropathol. *73:*365–369.

Panzica, G.C., R. Arévalo, F. Sánchez, J.R. Alonso, N. Aste, C. Viglietti-Panzica, J. Aijón, and R. Vázquez (1994) Topographical distribution of reduced nicotinamide adenine dinucleotide phosphate-diaphorase in the brain of the Japanese quail. J. Comp. Neurol. *342:*97–114.

Pearse, A.G.E. (1972) Principles of oxidoreductase histochemistry. In Histochemistry, Theoretical and Applied. Edinburgh: Churchill Livingstone, pp. 880–928.

Pinching, A.J. and T.P.S. Powell (1971) The neuron types of the glomerular layer of the olfactory bulb. J. Cell Sci. *9:*305–345.

Porteros, A., J.R. Alonso, R. Arévalo, E. García-Ojeda, C. Crespo, and J. Aijón (1994) Histochemical localization of NADPH-diaphorase in the rat accessory olfactory bulb. Chem. Senses *19:*413–424.

Price, J.L. and T.P.S. Powell (1970) The mitral and short axon cells of the olfactory bulb. J. Cell Sci. *7:*631–651.

Ramón y Cajal, S. (1904) Textura del Sistema Nervioso del Hombre y de los Vertebrados. Madrid: Imprenta de Nicolás Moya.

Rosene, D.L., N.J. Roy, and B.J. Davis (1986) A cryoprotection method that facilitates cutting frozen sections of whole monkey brains for histological and histochemical processing without freezing artifact. J. Histochem. Cytochem. *34:*1301–1315.

Sanides-Kohlrausch, C. and P. Wahle (1991) Distribution and morphology of substance P-immunoreactive structures in the olfactory bulb and olfactory peduncle of the common marmoset (*Callithrix jacchus*), a primate species. Neurosci. Lett. *131:*117–120.

Scott, J.W., J.K. McDonald, and J.L. Pemberton (1987) Short axon cells of the rat olfactory bulb display NADPH-diaphorase activity, neuropeptide Y-like immunoreactivity, and somatostatin-like immunoreactivity. J. Comp. Neurol. *260:*378–391.

Scott, J.W., D.P. Wellis, M.J. Riggott, and N. Buonviso (1993) Functional organization of the main olfactory bulb. Microsc. Res. Techn. *24:* 142–156.

Schneider, S.P. and F. Macrides (1978) Laminar distribution of interneurons in the main olfactory bulb of the adult hamster. Brain Res. Bull. *3:*73–82.

Serby, M., J. Corwin, P. Conrad, and J. Rotrosen (1985) Olfactory dysfunction in Alzheimer's disease and Parkinson's disease. Am. J. Psychiatry *142:*781–782.

Spessert, R., C. Wohlgemuth, S. Reuss, and E. Layes (1994) NADPH-diaphorase activity of nitric oxide synthase in the olfactory bulb: Co-factor specificity and characterization regarding the interrelation to NO formation. J. Histochem. Cytochem. *42:*569–575.

Stephan, H., and O.J. Andy (1970) The allocortex in primates. In C.R. Noback and W. Montagna (eds): The Primate Brain. New York: Appleton-Century Crofts, pp. 109–135.

Stewart, W.S., G.M. Kauer, and G.M. Shepherd (1979) Functional organization of rat olfactory bulb analyzed by 2-deoxyglucose method. J. Comp. Neurol. *185:*715–734.

Takagi, S.F. (1981) Multiple olfactory pathways in mammals. A review. Chem. Senses *6:*329–333.

Takagi, S.F. (1984) The olfactory nervous system of the Old World monkey. Jap. J. Physiol. *34:*561–573.

Takagi, S.F. (1986) Studies on the olfactory nervous system of the Old World monkey. Prog. Neurobiol. *27:*195–250.

Takeuchi, Y., H. Kimura, and Y. Sano (1982) Immunohistochemical demonstration of serotonin nerve fibers in the olfactory bulb of the rat, cat and monkey. Histochemistry *75:*461–471.

Talamo, B.R., W.-H. Feng, M. Perez-Cruet, L. Adelman, K. Kosik, V.M.-Y. Lee, L.C. Cork, and J.S. Kauer (1991) Pathological changes in olfactory neurons in Alzheimer's disease. Ann. N.Y. Acad. Sci. *640:*1–7.

Uemura, Y., N.W. Kowall, and M.F. Beal (1990) Selective sparing of NADPH-diaphorase-somatostatin-neuropeptide Y neurons in ischemic gerbil striatum. Ann. Neurol. *27:*620–625.

Villalba, R.M., R. Martínez-Murillo, I. Blasco, F.J. Alvarez, and J. Rodrigo (1988) C-PON containing neurons in the rat striatum are also positive for NADPH-diaphorase activity. A light microscopic study. Brain Res. *462:*359–362.

Villalba, R.M., J. Rodrigo, F.J. Alvarez, M. Achaval, and R. Martínez-Murillo (1989) Localization of C-PON immunoreactivity in the rat main olfactory bulb. Demonstration that the population of neurons containing endogenous C-PON display NADPH-diaphorase activity. Neuroscience *33:*373–382.

Vincent, S.R. and H. Kimura (1992) Histochemical mapping of nitric oxide synthase in the rat brain. Neuroscience *46:*755–784.